

ScienceDirect



IFAC PapersOnLine 56-2 (2023) 8260-8265

Cylinder Pressure Feedback Control for Ideal Thermodynamic Cycle Tracking: Towards Self-learning Engines

Maarten Vlaswinkel* Frank Willems*,**

* Control Systems Technology, Eindhoven University of Technology, Netherlands (email: m.g.vlaswinkel@tue.nl) ** TNO Automotive, Helmond, The Netherlands

Abstract: To meet increasingly strict future greenhouse gas and pollutant emission targets, development time and costs of heavy-duty internal combustion engines will reach unacceptable levels. This is mainly due to increased system complexity and need to guarantee robust performance under a wide range of real-world conditions. Cylinder Pressure Based Control is a major contributor to achieve these goals in advanced, highly-efficient engine concepts. Current Cylinder Pressure Based Control approaches use combustion and air-path parameters as feedback signals. These signals are not directly linked to engine efficiency; therefore, compensation for changing ambient conditions, engine ageing or differences in fuel qualities is a non-trivial problem. Contrary to other methods, the method presented in this paper aims to realise an idealised thermodynamic cycle by directly control of the entire cylinder pressure curve. From measured in-cylinder pressure, a new set of feedback signals is derived using principle component decomposition. With these signals, optimal fuel path settings are determined. The potential of this method is demonstrated for a dual fuel Reactivity Controlled Compression Ignition (RCCI) engine, which combines very high efficiency and ultra low nitrogen oxides and particle matter emission. For the studied RCCI engine, it is shown that the newly proposed optimisation method gave the same optimal fuel path settings as existing methods. This is an important step towards self-learning engines.

Copyright © 2023 The Authors. This is an open access article under the CC BY-NC-ND license (https://creativecommons.org/licenses/by-nc-nd/4.0/)

Keywords: Combustion control, Principal component analysis, Optimal control, Learning control, Engine calibration

1. INTRODUCTION

The transportation sector is a large contributor to the emission of greenhouse gasses and air pollutants (Jaramillo et al., 2022). Moving to a fully electrified heavy-duty transportation sector is, at the moment, not realistic for heavy transport with trucks and ships, or for heavy mining and construction machinery. Both the technology and the required infrastructure is not matured enough to facilitate this move. Therefore, the Internal Combustion Engine (ICE) will remain an important power source for heavy-duty applications in the upcoming decades. This requires ICEs to become cleaner, more efficient and is able to run on renewable fuels.

Effort has been made to adopt more advanced, Low Temperature Combustion (LTC) techniques (e.g. Homogenious Charge Compression Ignition, Partial Premixed Combustion and Reactivity Controlled Compression Ignition (RCCI) (Agarwal et al., 2017). While they promise high efficiency and low emissions, these results are only obtained in a controlled lab environment. Operation under a wide range of real-world conditions is one of the main challenges to get these type of ICEs production ready (Paykani et al., 2021). This entails making them more robust towards ageing, changing ambient conditions and difference in fuel quality. Furthermore, guarantees have to be in place, such that the combustion process is stable, as efficient as possible, and respects emission and mechanical safety constraints.

Cylinder Pressure Based Control (CPBC) is an important enabler for advanced, LTC techniques. It promises to improve combustion robustness, and enable safe and stable operation. With CPBC, the in-cylinder pressure is measured and used to determine appropriate control actions for the next combustion cycle (Willems, 2018). However, in current approaches the combustion process is indirectly controlled by predetermined setpoints of combustion and air-path characteristics (e.g., Irdmousa et al. (2021); Verhaegh et al. (2022)). These setpoints are, again, determined in a controlled lab environment. With these current approaches, robust performance can be guaranteed; however, it is impossible to give efficiency, emission and safety guarantees.

Efficiency, emission and safety guarantees are required, since LTC ICEs are sensitive to changing ambient conditions, ageing and differences in fuel quality. This can result in suboptimal efficiency or situations where emission or safety constraints are violated. To perform a lab calibration of all these different situations is not possible; it is too expensive and will require unacceptable development and test times. Therefore, self-learning techniques are required that automatically adapt control settings based on observed (suboptimal) behaviour and compensate for these unwanted effects in an online fashion (Willems, 2017). A few examples are found in the literature. Hinkelbein et al. (2012) present an Iterative Learning Control based method to directly compare a measure in-cylinder pressure to a predefined reference in-cylinder pressure of an RCCI

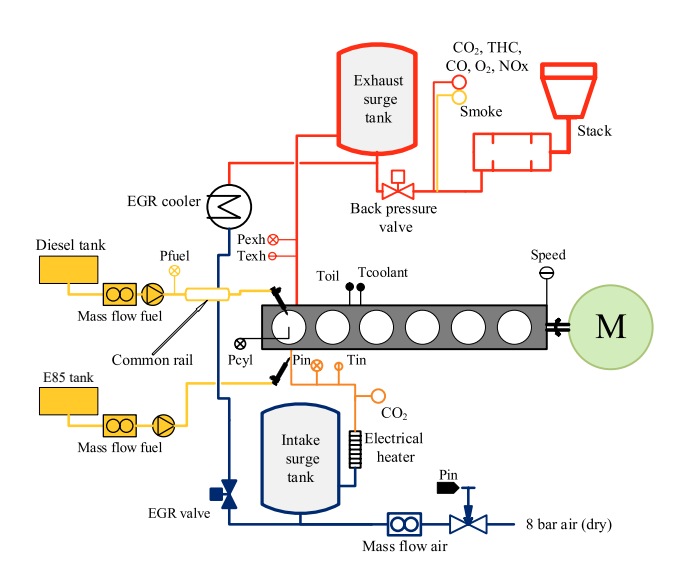


Fig. 1. Experimental six cylinder PACCAR MX13 engine equipped with a PFI-injector (Willems et al., 2020)

engine. However, no direct link to combustion efficiency can be made. van der Weijst et al. (2019) developed a combined fuel and air-path constrained extremum seeking control to optimise the brake specific fuel consumption of a heavy-duty Diesel engine. Guardiola et al. (2017) and Jorques Moreno et al. (2022) use heat release analysis to online optimisation of the indicated specific fuel consumption and indicate efficiency of a Diesel engine. However, non of these methods is able to control a complete incylinder pressure and only track specific combustion characteristics.

In this paper, a novel energy-based CPBC approach applied to an RCCI engine will be presented. Efficiency and safety consideration are directly linked to the in-cylinder pressure in a way that is applicable to a large range of control methods. Pan et al. (2019) and Vlaswinkel et al. (2022) used Principle Component Decomposition (PCD) to model in-cylinder pressures, and Chung et al. (2017) used PCD as an in-cylinder pressure noise filter. In this paper, PCD is used to formulate a new feedback control approach. The Otto cycle, an Idealised Thermodynamic Cycle (ITC), is used as a reference. It will be shown that this new metric directly links to the efficiency of the combustion process and safety constraints. This paper will not go into the robustness problem, but it is believed that the approaches mentioned before can be adapted to use the proposed metric.

The structure of this paper is as follows. First, the general control problem is described and a brief overview is given of the state-of-the-art control method. Thereafter, a novel energy based control method is presented followed by some simulation results.

2. CONTROL PROBLEM

In the following study an RCCI engine running on Diesel and E85 will be used. Fig. 1 shows the used six cylinder PACCAR MX13 engine available in the Zero-Emission Lab of the Eindhoven University of Technology. Only cylinder 1 is active. The cylinder heads of cylinders 2-6 have been removed and no fuel is injected into these cylinders. The cylinder pressure of cylinder 1 is measured using a Kistler 6125C. To enable RCCI operation, the engine uses a direct injection system to inject diesel directly into the cylinder

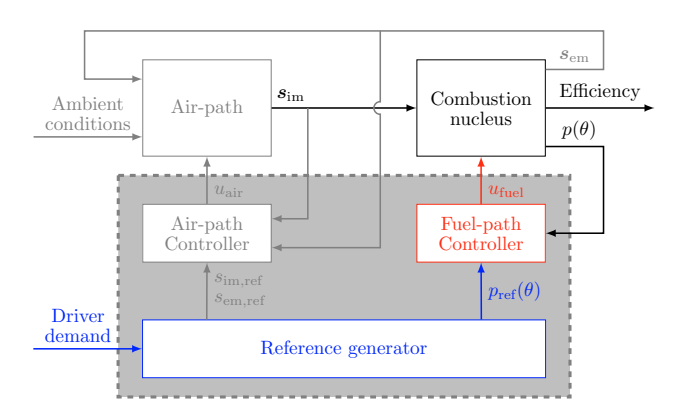


Fig. 2. General engine control scheme with reference generator and separate air and fuel-path controllers, where $s_{\rm im}$ and $s_{\rm em}$ are the conditions at the intake and exhaust manifold, $u_{\rm air}$ and $u_{\rm fuel}$ are the inputs to the air and fuel path actuators and $p(\theta)$ is the measured in-cylinder pressure.

and a port fuel injection system to inject E85 in the intake port. An electric machine is used to generate the torque required to keep the engine running at a constant speed.

A general ICE control scheme for the fuel and air-path is shown in the gray area of Fig. 2. The main goal of this engine controller is to realise the requested power with maximal thermal efficiency, while meeting tailpipe emission limits and guarantying safe operation. In this paper, the focus is on the fuel-path controller. Three controlled inputs are available in the studied engine. To control the requested power, the total injected fuel energy is used:

$$Q_{\text{fuel}} = m_{\text{PFI}} LHV_{\text{PFI}} + m_{\text{DI}} LHV_{\text{DI}}, \tag{1}$$

where $m_{\rm PFI}$ and $m_{\rm DI}$ are the mass of Port Fuel Injected (PFI) and Direct Injected (DI) fuels and LHV_{PFI} and LHV_{DI} the lower heating value of these fuels, respectively. Second, the energy based Blend Ratio (BR)

$$BR := \frac{m_{PFI}LHV_{PFI}}{Q_{\text{fuel}}}$$
 (2)

is used to control the in-cylinder fuel reactivity. Third, the start-of-injection of the directly injected fuel ${\rm SOI_{DI}}$ affects combustion phasing.

To evaluate thermal efficiency, in this work we focus on the gross indicated efficiency

GIE
$$(u_{\text{fuel}}, s_{\text{im}}) := \frac{1}{Q_{\text{fuel}}} \int_{\Theta} p(\theta, u_{\text{fuel}}, s_{\text{im}}) dV(\theta),$$
 (3)

with cylinder pressure $p(\theta, u)$, cylinder volume $V(\theta)$ and crank angle $\Theta = [-180\,\text{CAD}, \, 180\,\text{CAD}]$ with focus on the high pressure part of the four stroke engine cycle. To limit mechanical stresses and combustion noise, peak pressure and peak pressure rise rate are constrained by, respectively:

$$p_{\max} := \max_{\theta} p(\theta) \tag{4}$$

and

$$\left(\frac{dp}{d\theta}\right)_{\max} := \max_{\theta} \left(\frac{dp}{d\theta}\right) \tag{5}$$

Using (3) to (5), the optimisation problem during engine calibration can be formulated as

$$u^* = \underset{u \in \mathcal{U}}{\operatorname{arg\,max}} \quad \operatorname{GIE}(u)$$
s.t.
$$p_{\max} < p_{\max, \mathrm{ub}}$$

$$\left(\frac{dp}{d\theta}\right)_{\max} < \left(\frac{dp}{d\theta}\right)_{\max, \mathrm{ub}},$$
(6)

where $u \in \mathcal{U}$ is the inputs to the system and \mathcal{U} the input domain, and $p_{\text{max,ub}}$ and $\left(\frac{dp}{d\theta}\right)_{\text{max,ub}}$ the allowed upper bound of the peak pressure and peak pressure rise rate.

3. STATE-OF-THE-ART CYLINDER PRESSURE BASED CONTROL

A common way to define the feedback control problem is to use the feedback error as $e=x-x_{\rm ref}$, where x and $x_{\rm ref}$ are vectors consisting of measured and references of combustion related parameters, respectively (Willems, 2018). For combustion control, traditionally, the metrics in x show good correlations with the high level objectives z, such as thermal efficiency and emissions. These metrics are often based on a measured in-cylinder pressure signal. Examples of such high level objectives and related metrics are given in Table 1.

Besides the peak pressure and peak pressure rise rate in (4) and (5), the net indicated mean effective pressure, which is a measure for the power output, is often determined:

$$IMEP_n := IMEP_{\mathfrak{G}}(u) - PMEP$$
 (7)

with gross indicated mean effective pressure:

IMEP_g(
$$u_{\text{fuel}}, s_{\text{im}}$$
) := $\frac{1}{V_{\text{d}}} \int_{\Theta} p(\theta, u_{\text{fuel}}, s_{\text{im}}) dV(\theta)$, (8)

and with pumping mean effective pressure:

$$\text{PMEP} := \frac{1}{V_{\rm d}} \left(\int_{-360 \, {\rm CAD}}^{-180 \, {\rm CAD}} p(\theta) \, dV(\theta) + \int_{180 \, {\rm CAD}}^{360 \, {\rm CAD}} p(\theta) \, dV(\theta) \right) \ \, \left(9 \right)$$

where $V_{\rm d}$ is the displacement volume.

Moreover, the apparent rate of heat release can be derived from the in-cylinder pressure as

$$aROHR(\theta) := \frac{\gamma(\theta)}{\gamma(\theta) - 1} p(\theta) \frac{dV}{d\theta} + \frac{1}{\gamma(\theta) - 1} V(\theta) \frac{dp}{d\theta}, (10)$$

where $\gamma(\theta)$ is the temperature and composition dependent specific heat ratio. Using (10), the cumulative heat release is found by

$$HR(\theta) := \int_{-180 \text{ CAD}}^{\theta} aROHR(\theta) d\theta.$$
 (11)

This heat release is used to compute combustion phasing metrics: e.g., start of combustion (SOC), crank angle at 50% of heat released (CA50) and combustion duration (CA90-CA10).

Table 1. Examples of combustion metrics used for indirect control of high level objectives

High level objective z	Combustion metric x
Efficiency	Crank angle at 50% of heat released CA50 Pressure difference across engine Δp Pumping loss PEMP, Air-to fuel ratio λ
Emissions	Energy based BR, EGR fraction X_{EGR}
Combustion stability	Energy based BR, Intake manifold temperature $T_{\rm im}$
Safety	$p_{ m max}$ and $\left(rac{dp}{d heta} ight)_{ m max}$
Power output	Indicated mean effective pressure (IMEP)

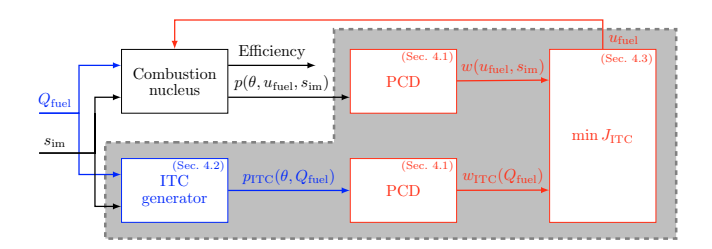


Fig. 3. Schematic of the proposed fuel-path control architecture with Principle Component Decomposition (PCD) and an Idealised Thermodynamic Cycle (ITC) to regulate the combustion nucleus, where the colour scheme corresponds with Fig. 2

The reference vector $x_{\rm ref}$ is typically determined offline by calibration experts who tries to solve (6) over the full operating range. The found reference vectors $x_{\rm ref}$ are stored into a fixed map. As a result, efficiency and emissions are controlled indirectly by controlling x. This approach requires the correlation z(x) to be known and assumes that the effect of changes in these correlations on control performance are negligible.

4. SELF-LEARNING FUEL PATH CONTROL

In this section, a novel feedback method is presented that uses an energy based approach to control the fuel parameters. A schematic overview of the control architecture is shown in Fig. 3. It uses a PCD of the pressure trace, which is as often used to filter out measurement noise (Chung et al., 2017) and create data-based cylinder pressure models (Pan et al., 2019; Vlaswinkel et al., 2022). This decomposition reduces the dimensions of the pressure trace to $n_{\rm PC} \in \mathbb{N}_{>0}$ values, where $n_{\rm PC}$ is the number of used Principle Components (PCs). It will be shown that this decomposition can be used to formulate an energy based cost function using a measure cylinder pressure and idealised thermodynamic cycle.

4.1 Principle Component Decomposition of In-cylinder Pressure

The decomposition of the pressure trace in PCs is done using PCD. The measured cylinder pressure is decomposed as

 $p(\theta, u_{\text{fuel}}, s_{\text{im}}) = w(u_{\text{fuel}}, s_{\text{im}})^{\mathsf{T}} f(\theta) + f_{\mu}(\theta) + \epsilon(\theta), \quad (12)$ where $w(u_{\text{fuel}}, s_{\text{im}}) \in \mathbb{R}^{n_{\text{PC}}}$ is a vector of weights, $f(\theta) \in \mathbb{R}^{n_{\text{PC}}}$ is the vector of PCs, $f_{\mu}(\theta) \in \mathbb{R}$ is the average observed cylinder pressure over the whole operating range and $\epsilon(\theta) \in \mathbb{R}$ is the residual between measured and modelled cylinder pressure.

To determine the PCs, $n_e \in \mathbb{N}_{>0}$ experiments at different fuel and intake manifold conditions are performed. During each experiments, the cylinder pressure $\boldsymbol{p} \in \mathbb{R}_{>0}^{n_{\text{CA}}}$ at $n_{\text{CA}} \in \mathbb{N}_{>0}$ crank angle positions for $n_c \in \mathbb{N}_{>0}$ cycles is recorded. All experiments are then combined into a matrix $P \in \mathbb{R}_{>0}^{n_e n_c \times n_{\text{CA}}}$. Using P, the average observed cylinder pressure and PCs are given by

$$f_{\mu}(\theta_j) := \frac{1}{n_{\rm e} n_{\rm c}} \sum_{i=1}^{n_{\rm e} n_{\rm c}} P_{ij}$$
 (13)

and $f(\theta)$ are the first n_{PC} eigen vectors of $(P - f_{\mu})^{\mathsf{T}}(P - f_{\mu})$.

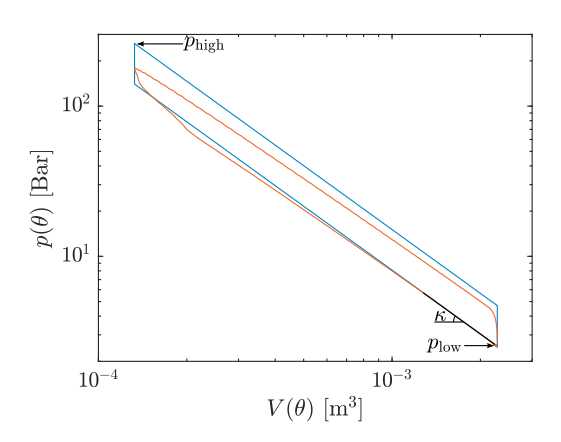


Fig. 4. The pV-diagram of a measured in-cylinder pressure (-) and the corresponding idealised thermodynamic Otto cycle (-)

Deviating from standard PCD, a work based approach is used to determine w(u). The goals is to minimise the size of the area of the residual in the pV-diagram as

$$w^{*}(u_{\text{fuel}}, s_{\text{im}}) = \underset{w \in \mathbb{R}^{n_{\text{PC}}}}{\operatorname{arg \, min}} \int_{\Theta} \left| \epsilon(\theta) \frac{dV}{d\theta} \right| d\theta,$$
$$= \underset{w \in \mathbb{R}^{n_{\text{PC}}}}{\operatorname{arg \, min}} \int_{\Theta} \epsilon(\theta)^{2} \left(\frac{dV}{d\theta} \right)^{2} d\theta. \tag{14}$$

Substituting (12) into (14), this become

$$w(u_{\text{fuel}}, s_{\text{im}}) = \underset{v \in \mathbb{R}^{n_{\text{PC}}}}{\arg\min} v^{\mathsf{T}} \int_{\Theta} f(\theta) f^{\mathsf{T}}(\theta) \left(\frac{dV}{d\theta}\right)^{2} d\theta \ v + \\ v^{\mathsf{T}} \int_{\Theta} f(\theta) \left(f_{\mu}(\theta) - p(\theta, u_{\text{fuel}}, s_{\text{im}})\right) \left(\frac{dV}{d\theta}\right)^{2} d\theta$$
(15)

This problem can be algebraically solved as

$$w(u_{\text{fuel}}, s_{\text{im}}) = -A_1 A_2^{-1} \tag{16}$$

with

$$A_{1} = \int_{\Theta} f(\theta) \left(f_{\mu}(\theta) - p(\theta, u_{\text{fuel}}, s_{\text{im}}) \right) \left(\frac{dV}{d\theta} \right)^{2} d\theta$$

and

$$A_2 = \int_{\Theta} f(\theta) f^{\mathsf{T}}(\theta) \left(\frac{dV}{d\theta} \right)^2 d\theta.$$

4.2 Idealised Thermodynamic Cycle

In this paper, an ITC is used. The Otto cycle is chosen because it promises the highest thermal efficiency over a large operating range (Heywood, 2018). It is a combination of two isentropic and two isochoric processes as shown in Fig. 4. It can be fully described by the Q_{fuel} , pressure at the start of the compression stroke p_{low} , the cylinder volume over time $V(\theta)$ and temperature and composition dependent specific heat ratio γ . The air-path is mostly responsible for p_{low} and γ . The Otto cycle is given by

$$p_{\text{ITC}}(\theta, Q_{\text{fuel}}, s_{\text{im}}) = \begin{cases} p_{\text{low}} \left(\frac{V(-180 \,\text{CAD})}{V(\theta)} \right)^{\gamma}, & \text{if } \theta \in \Theta_{\text{c}}, \\ p_{\text{high}} \left(\frac{V(0 \,\text{CAD})}{V(\theta)} \right)^{\gamma}, & \text{if } \theta \in \Theta_{\text{e}} \end{cases}$$
(17)

with $\Theta_c = [-180 \text{ CAD}, 0 \text{ CAD}], \Theta_e = [0 \text{ CAD}, 180 \text{ CAD}],$

$$p_{\text{high}} = \frac{\eta_{\text{ITC}} Q_{\text{fuel}} - \int_{-180 \text{ CAD}}^{0 \text{ CAD}} p_{\text{ITC}}(\theta, Q_{\text{fuel}}) dV}{V^{\gamma}(0 \text{ CAD}) \int_{-180 \text{ CAD}}^{0 \text{ CAD}} V^{-\gamma}(\theta) dV(\theta)}$$

and efficiency of the Otto cycle $\eta_{\rm ITC}$ is given by

$$\eta_{\rm ITC} = 1 - \frac{1}{r^{\gamma - 1}} \tag{18}$$

with $r = \max(V) \min(V)^{-1}$ the compression ratio. Using (18), it is found that the thermal efficiency increases when γ increases.

The cylinder pressure decomposition presented in Sec. 4.1 is also used to decompose $p_{\text{ITC}}(\theta, Q_{\text{fuel}})$.

4.3 Minimisation of energy losses

During a combustion cycle, the energy is conserved. This means

$$W_{\text{ind }\sigma} = IMEP_{\sigma}V_{\text{d}} = Q_{\text{fuel}} + Q_{\text{loss}},$$
 (19)

 $W_{\rm ind,g} = IMEP_{\rm g}V_{\rm d} = Q_{\rm fuel} + Q_{\rm loss}, \qquad (19)$ where $W_{\rm ind,g}$ is the gross indicated work applied to the piston and $Q_{\rm loss}$ are the total energy losses. These losses are split into two parts: i) the energy loss obtained when running a perfect Otto cycle and (ii) the additionally energy losses Q_{NITC} associated with a non-ideal cycle. Using (18), this can be written as

$$Q_{\text{loss}} = (1 - \eta_{\text{ITC}})Q_{\text{fuel}} + Q_{\text{NITC}}.$$
 (20)

Substituting (20) into (19) gives

$$Q_{\rm NITC} = W_{\rm ind,g} - \eta_{\rm ITC} Q_{\rm fuel}.$$
 (21)

Given a measured cylinder pressure $p(\theta)$ and Otto cycle $p_{\rm ITC}(\theta)$, $Q_{\rm NITC}$ can be computed by

$$Q_{\text{NITC}} = \int_{\Theta} \left(p(\theta, u) - p_{\text{ITC}}(\theta) \right) dV(\theta)$$
 (22)

The goal is to reduce the size this loss; therefore, the cost function is defined as

$$J = Q_{\text{NITC}}^2 = \left(\int_{\Theta} \left(p(\alpha, u) - p_{\text{ITC}}(\alpha) \right) dV(\theta) \right)^2. \tag{23}$$

Using the decomposition of (12) to decompose $p(\theta)$ and $p_{\rm ITC}$, (23) can be rewritten as

$$J = \left(\int_{\Theta} w(u_{\text{fuel}}, s_{\text{im}})^{\mathsf{T}} f(\theta) + f_{\mu}(\theta) + \epsilon(\theta) dV - \int_{\Theta} w_{\text{ITC}}^{\mathsf{T}} f(\theta) + f_{\mu}(\theta) + \epsilon_{\text{ITC}}(\theta) dV \right)^{2},$$

$$= (w(u_{\text{fuel}}, s_{\text{im}}) - w_{\text{ITC}})^{\mathsf{T}} Z_{1}(w(u_{\text{fuel}}, s_{\text{im}}) - w_{\text{ITC}}) + 2(w(u_{\text{fuel}}, s_{\text{im}}) - w_{\text{ITC}})^{\mathsf{T}} Z_{2} + Z_{3}$$

$$(24)$$

with

$$Z_1 = \iint_{\Theta} f(\theta_1) f^{\mathsf{T}}(\theta_2) \, dV(\theta_1) \, dV(\theta_2),$$
$$Z_2 = \iint_{\Theta} f(\theta_1) (\epsilon(\theta_2) - \epsilon_{\mathrm{ITC}}(\theta_2)) \, dV(\theta_1) \, dV(\theta_2)$$

$$Z_3 = \iint_{\Theta} (\epsilon(\theta_1) - \epsilon_{\mathrm{ITC}}(\theta_1)) (\epsilon(\theta_2) - \epsilon_{\mathrm{ITC}}(\theta_2)) \ dV(\theta_1) \ dV(\theta_2).$$
 The weights w and w_{ITC} are determined such that $\int_{\Theta} \epsilon(\theta)^2 \ dV(\theta)$ and $\int_{\Theta} \epsilon_{\mathrm{ITC}}(\theta)^2 \ dV(\theta)$ are minimised. When enough PCs are used these terms will approach 0; therefore, it can be assumed that $Z_2 \approx 0$ and $Z_3 \approx 0$. This reduces (24) to

$$J \approx J_{\text{ITC}} = (w(u) - w_{\text{ITC}})^{\mathsf{T}} Z_1(w(u) - w_{\text{ITC}}).$$
 (25)

The original control problem in (6) also contains constraints. Using (12), these can be rewritten as linear constraints as

$$w(u)^{\mathsf{T}} f(\theta) + f_{\mu}(\theta) < p_{\text{max,ub}}, \ \forall \theta \in \Theta$$
 (26)

and

$$w(u)^{\mathsf{T}} \frac{df}{d\theta} + \frac{df_{\mu}}{d\theta} < \left(\frac{dp}{d\theta}\right)_{\text{max,ub}}, \ \forall \theta \in \Theta$$
 (27)

where again it is assumed that the residual $\epsilon(\theta)$ can be neglected.

Using (25) until (27), the original control problem of (6) can be reformulated as

$$u^* = \underset{u \in \mathcal{U}}{\operatorname{arg \, min}} \quad (w(u) - w_{\text{ITC}})^{\mathsf{T}} Z_1(w(u) - w_{\text{ITC}})$$
s.t.
$$w(u)^{\mathsf{T}} f(\theta) + f_{\mu}(\theta) < p_{\text{max,ub}}, \ \forall \theta \in \Theta$$

$$w(u)^{\mathsf{T}} \frac{df}{d\theta} + \frac{df_{\mu}}{d\theta} < \left(\frac{dp}{d\theta}\right)_{\text{max,ub}}, \ \forall \theta \in \Theta,$$

$$(28)$$

This means that the control problem has been reformulated into a quadratic cost function and linear constraints in terms of w(u).

5. SIMULATION RESULTS

In this section, a simulation study is performed using the same setup and experimental data as in Willems et al. (2020). Below only the most relevant information is provided. Table 2 shows the engine specifications and nominal operating conditions. The experimental data consist of 988 different experiments using different intake manifold pressures, start of injection of Diesel, and mass of injected Diesel and E85. Each experiment consist of 200 consecutive combustion cycles. As a proof of concept, these consecutive combustion cycles have been averaged into one average combustion cycle $\bar{p}(\theta, u_{\rm fuel}, s_{\rm im})$ to reduce the effect of sensor and actuator noise.

Using the experimental data, the PCs are determined according to Sec. 4.1 with $n_{\rm PC}=7$. The weights w(u) of the measured pressure traces is given in (16). The corresponding Otto cycle is determined by setting $p_{\rm low}=\bar{p}(-180\,{\rm CAD},\,u_{\rm fuel},\,s_{\rm im})$ and IMEP_{g,ref} = $V_{\rm d}^{-1}\int_{\Theta}\bar{p}(\theta)\,dV(\theta)$. The specific heat ratio $\gamma(s_{\rm im})$ is determined using the measured cylinder pressure $\bar{p}(\theta,\,u_{\rm fuel},\,s_{\rm im})$ as

$$\gamma(s_{\rm im}) = \frac{\ln \bar{p}(\theta_1, u_{\rm fuel}, s_{\rm im}) - \ln \bar{p}(\theta_2, u_{\rm fuel}, s_{\rm im})}{\ln V(\theta_2) - \ln V(\theta_1)}, \quad (29)$$

where $\theta_1, \theta_2 \in [\theta_{\text{IVC}}, \theta_{\text{SOI}}]$ and $\theta_1 < \theta_2$ with θ_{IVC} the crank angle where the intake valve closes. In the following discussion, it is chosen that $\theta_1 = -160\,\text{CAD}$ and $\theta_2 = -100\,\text{CAD}$. Using (17), the full Otto cycle $p_{\text{ITC}}(\theta,\,Q_{\text{fuel}})$ is computed. The Otto cycle $p_{\text{ITC}}(\theta,\,Q_{\text{fuel}})$ is decomposed using the previously determined PCs and (16).

Fig. 5 shows that $J_{\rm ITC}$ and the GIE are linked. An increase in efficiency results in a decrease of $J_{\rm ITC}$. Therefore,

Table 2. Specifications and nominal operating conditions of the engine setup and range of u_{fuel} and s_{im} used during the experiments

Parameters	Value
PFI fuel	E85
DI fuel	Diesel (EN590)
Compression ratio	17.2
Intake valve closure	$-173^{\circ}\text{CA aTDC}$
Exhaust valve opening	$146^{\circ}\text{CA aTDC}$
Gross IMEP	$(8.5 \pm 1.0) \mathrm{bar}$
Engine speed	1200 rpm
Crank angle resolution	$0.2\mathrm{CAD}$
$p_{ m max,ub}$	$200\mathrm{Bar}$
$\left(\frac{dp}{d\theta}\right)_{\text{max,ub}}$	$25\mathrm{Bar/CAD}$
BR	[0.76, 0.81]
$Q_{ m fuel}$	[3815, 4107] J/cycle
SOI_{DI}	[-70, -35] CAaTDC
$p_{ m im}$	$[2.18, 2.53] \cdot 10^5 \mathrm{Pa}$
$T_{ m im}$	$[270, 320.5] \mathrm{K}$

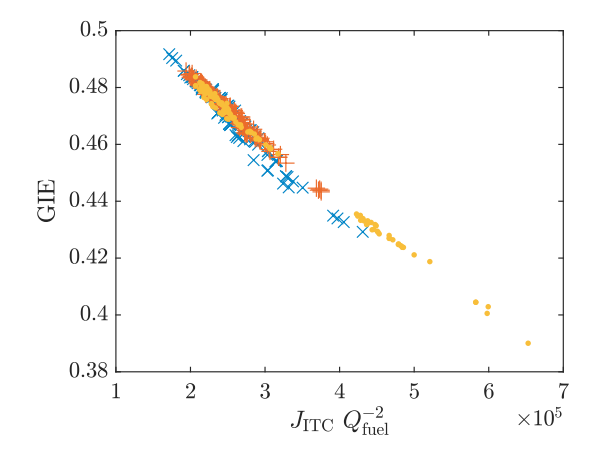


Fig. 5. Energy based cost function $J_{\rm ITC}$ as given in (25) scaled with $Q_{\rm fuel}^2$ with $n_{\rm PC}=7$ against Gross Indicate Efficiency (GIE) with intake manifold pressures of (2.100 ± 0.025) bar (\times) , (2.300 ± 0.025) bar (+), and (2.500 ± 0.025) bar (\cdot) .

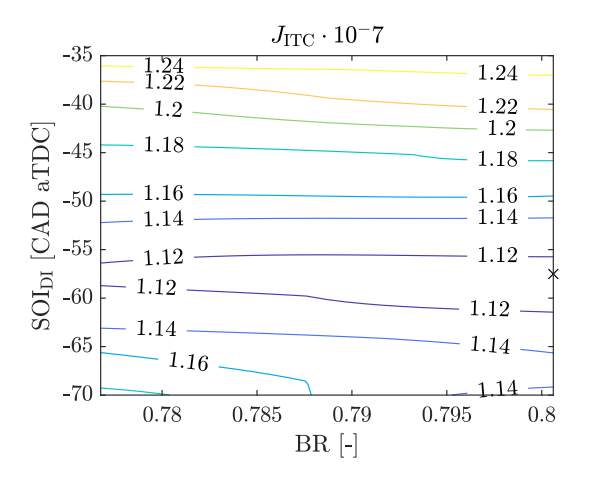


Fig. 6. Contour plot of $J_{\rm IVC}$ at $Q_{\rm fuel}=3966.8\,{\rm J}$ and intake manifold pressure set to $2.3\cdot 10^5\,{\rm Pa}$ and intake temperature to 306 K evaluate over the allowed input space. The minimum is marked with an '×'

 $J_{\rm ITC}$, as formulated in (25), can be used to optimise the thermal efficiency. Moreover, $p_{\rm im}$ only has a minimal effect on the GIE. The effect of $p_{\rm im}$ on the overall efficiency mainly enters though pumping losses not included in this discussion.

The original optimisation problem of (6) and newly formulated optimisation problem of (28) using an idealised thermodynamic cycle are solved for a range of fuel energies $Q_{\rm fuel}$ and constant intake manifold condition. The in-cylinder pressure model using Gaussian Process Regression presented by Vlaswinkel et al. (2022), MATLAB R2022a and the constrained non-linear solver using the interior-point method and a random multi-start approach found in the Optimisation Toolbox are used to solve the optimisation problem. The intake manifold pressure is set to 2.3 Bar, intake temperature to 306 K and γ to 1.33 averagely observed on the setup using (29). Fig. 6 shows the contour plot of $J_{\rm ITC}$ over the input space for $Q_{\rm fuel}=3966.8\,\rm J$. It can be seen that $J_{\rm ITC}$ is mostly sensitive toward SOI_{DI} in the shown range. Solving (6) and (28) for all studied $Q_{\rm fuel}$, the optimal GIE, BR and SOI_{DI} shown in Fig. 7 are found. In this figure, it can be seen

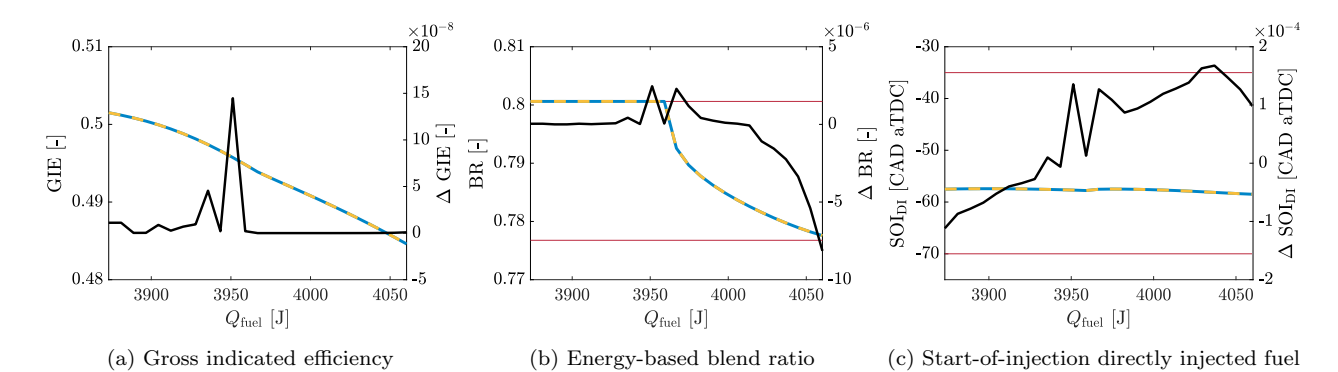


Fig. 7. Resulting GIE, BR and SOI_{DI} with intake manifold pressure set to $2.3 \cdot 10^5$ Pa and intake temperature to $306 \,\mathrm{K}$ when solving the original optimisation problem of (6) (--), the optimisation problem based on an idealised thermodynamic cycle of (28) (--) and the difference between the two methods (-). The upper and lower bound of the inputs are shown in red.

that both methods produce slightly different values for the inputs, but these difference are to small to be reproduced on a real system. Therefore, both methods result in the same inputs.

6. CONCLUSIONS

In this paper, a novel energy-based cylinder pressure feedback formulation has been proposed. It uses an ITC as reference; thereby, providing a formulation that is inline with a large range of feedback control methods. Furthermore, the proposed method provides a direct link with thermal efficiency and safety constraints. Hereby promising more optimal performance during operation. Simulated experiments show that the same GIE and fuel inputs are reached when optimising over the GIE or towards an ITC.

In future work emission constraints will be added to the optimisation problem. Henningsson et al. (2012) proposes a method that uses Principle Component Analysis (PCA) and a neural network to predict emission values based on the weights w(u). This methods fits well with the method proposed in this paper. Furthermore, the pumping loop will be incorporated to include pumping losses and provide the ability to optimise over the net indicated efficiency.

ACKNOWLEDGEMENTS

The research presented in this paper is financially supported by the Dutch Technology Foundation (STW) under project number 14927. The authors would like to thank Robbert Willems for making the experimental data available during this project.

REFERENCES

Agarwal, A.K., Singh, A.P., and Maurya, R.K. (2017). Evolution, challenges and path forward for low temperature combustion engines. Progress in Energy and Combustion Science, 61, 1–56. doi: 10.1016/j.pecs.2017.02.001.

Chung, J., Oh, J., and Sunwoo, M. (2017). A Real-Time Combustion Control With Reconstructed In-Cylinder Pressure by Principal Component Analysis for a CRDI Diesel Engine. *Journal of Engineering* for Gas Turbines and Power, 139(062802). doi:10.1115/1.4035395. Number: 062802.

Guardiola, C., Climent, H., Pla, B., and Reig, A. (2017). Optimal Control as a method for Diesel engine efficiency assessment including pressure and NO x constraints. *Applied Thermal Engineering*, 117, 452–461. doi:10.1016/j.applthermaleng.2017.02.056.

Henningsson, M., Tunestål, P., and Johansson, R. (2012). A Virtual Sensor for Predicting Diesel Engine Emissions from Cylinder Pressure Data. IFAC Proceedings Volumes, 45(30), 424–431. doi: 10.3182/20121023-3-FR-4025.00063. Number: 30.

Heywood, J.B. (2018). Internal Combustion Engine Fundamentals, Second Edition. McGraw-Hill Education.

Hinkelbein, J., Kremer, F., Lamping, M., Körfer, T., Schaub, J., and Pischinger, S. (2012). Experimental realisation of predefined diesel combustion processes using advanced closed-loop combustion control and injection rate shaping. *International Journal of Engine Re*search, 13(6), 607–615. doi:10.1177/1468087412439262. Number: 6 Publisher: SAGE Publications.

Irdmousa, B.K., Naber, J.D., Velni, J.M., Borhan, H., and Shahbakhti, M. (2021). Input-output Data-driven Modeling and MIMO Predictive Control of an RCCI Engine Combustion. *IFAC-PapersOnLine*, 54(20), 406–411. doi:10.1016/j.ifacol.2021.11.207. Number: 20.

Jaramillo, P., Kahn Ribeiro, S., Newman, P., Dhar, S., Diemuodeke, O., Kajino, T., Lee, D., Nugroho, S., Ou, X., Strømman, H., and Whitehead, J. (2022). Chapter 10: Transport. In IPCC, 2022: Climate Change 2022: Mitigation of Climate Change. Contribution of Working Group III to the Sixth Assessment Report of the Intergovernmental Panel on Climate Change.

Jorques Moreno, C., Stenlåås, O., and Tunestål, P. (2022). Indicated efficiency optimization by in-cycle closed-loop combustion control of diesel engines. Control Engineering Practice, 122, 105097. doi: 10.1016/j.conengprac.2022.105097.

Pan, W., Korkmaz, M., Beeckmann, J., and Pitsch, H. (2019). Unsupervised learning and nonlinear identification for in-cylinder pressure prediction of diesel combustion rate shaping process. IFAC-PapersOnLine, 52(29), 199–203. doi:10.1016/j.ifacol.2019.12.644. Number: 29.

Paykani, A., Garcia, A., Shahbakhti, M., Rahnama, P., and Reitz, R.D. (2021). Reactivity controlled compression ignition engine: Pathways towards commercial viability. Applied Energy, 282, 116174. doi: 10.1016/j.apenergy.2020.116174.

van der Weijst, R., van Keulen, T., and Willems, F. (2019). Constrained multivariable extremum-seeking for online fuel-efficiency optimization of Diesel engines. *Control Engineering Practice*, 87, 133–144. doi: 10.1016/j.conengprac.2019.03.008.

Verhaegh, J., Kupper, F., and Willems, F. (2022). Data-Driven Air-Fuel Path Control Design for Robust RCCI Engine Operation. *Energies*, 15(6), 2018. doi:10.3390/en15062018. Number: 6 Publisher: Multidisciplinary Digital Publishing Institute.

Vlaswinkel, M., de Jager, B., and Willems, F. (2022). Data-Based In-Cylinder Pressure Model including Cyclic Variations of an RCCI Engine. IFAC-PapersOnLine, 55(24), 13–18. doi: 10.1016/j.ifacol.2022.10.255.

Willems, F. (2017). The self-learning powertrain: towards smart and green transport. Technische Universiteit Eindhoven, Eindhoven.

Willems, F. (2018). Is Cylinder Pressure-Based Control Required to Meet Future HD Legislation? IFAC-PapersOnLine, 51(31), 111–118. doi: 10.1016/j.ifacol.2018.10.021. Number: 31.

Willems, R., Willems, F., Deen, N., and Somers, B. (2020). Heat release rate shaping for optimal gross indicated efficiency in a heavyduty RCCI engine fueled with E85 and diesel. Fuel, 119656. doi: 10.1016/j.fuel.2020.119656.